Biochemical and Biophysical Research Communications 454 (2014) 172–177

Contents lists available at ScienceDirect

Biochemical and Biophysical Research Communications

journal homepage: www.elsevier.com/locate/ybbrc

Nuclear lactate dehydrogenase modulates histone modification in human hepatocytes

Zachary Castonguay, Christopher Auger, Sean C. Thomas, M'hamed Chahma, Vasu D. Appanna *

Department of Chemistry and Biochemistry, Laurentian University, Sudbury, Ontario P3E 2C6, Canada

ARTICLE INFO

Article history:
Received 6 October 2014
Available online 18 October 2014

Keywords:
Metabolism
Epigenetics
Lactate dehydrogenase
Sirtuin
Oxidative stress

ABSTRACT

It is becoming increasingly apparent that the nucleus harbors metabolic enzymes that affect genetic transforming events. Here, we describe a nuclear isoform of lactate dehydrogenase (nLDH) and its ability to orchestrate histone deacetylation by controlling the availability of nicotinamide adenine dinucleotide (NAD^+), a key ingredient of the sirtuin-1 (SIRT1) deacetylase system. There was an increase in the expression of nLDH concomitant with the presence of hydrogen peroxide (H_2O_2) in the culture medium. Under oxidative stress, the NAD^+ generated by nLDH resulted in the enhanced deacetylation of histones compared to the control hepatocytes despite no discernable change in the levels of SIRT1. There appeared to be an intimate association between nLDH and SIRT1 as these two enzymes co-immunoprecipitated. The ability of nLDH to regulate epigenetic modifications by manipulating NAD^+ reveals an intricate link between metabolism and the processing of genetic information.

1. Introduction

The long-accepted central dogma in the flow of biological information dictates that a protein is translated from an RNA sequence stemming from DNA. However, recent discoveries have begun to shed some light on the pivotal role proteins and metabolites play in the translation of genetic information. Nowhere is this more apparent than in the dynamic modifications regulating chromatin, the guardian of genetic material. Indeed, it is well known that the activity of histone acetyltransferases (HATs) is dependent on the nuclear concentration of their key substrate, acetyl-CoA, a feature controlled by a nuclear isoform of adenosine triphosphate (ATP) – citrate lyase (nACL) [1]. The availability of this moiety favors the acetylation of histones, a biochemical event responsible for the modulation of gene expression. Histone deacetylases (HDACs), also referred to as sirtuins, on the other hand mediate the removal of the acetyl group from histones, a situation also associated with the manipulation of genetic information [2].

One group of sirtuins (class III HDACs) in particular are dependent on NAD^+ hydrolysis for catalytic activity, thus linking the translation of genetic information to metabolic cues within the cell, either in the nucleus or other organelles. These crucial enzymes are sensitive to NAD^+ concentrations in the nucleus and are associated with such human disorders as diabetes, cancer and neurodegenerative diseases [3–5]. Of the sirtuins discovered so far, SIRT1 is likely the best characterized, and is involved in regulating gene expression via its direct interaction with histones, transcription factors, components of the transcriptional machinery and other proteins [6,7]. Studies have shown that the NAD^+ requirements of this enzyme are fulfilled by the NAD^+ salvage pathway, consisting of the enzymes nicotinamide mononucleotide adenyltransferase (NMNAT) and nicotinamide phosphoribosyltransferase (NAMPT) [8,9]. Indeed, increased activity of the latter through environmental stimuli has been correlated to SIRT1-mediated changes in gene regulation [10].

The localization of metabolic enzymes in different cellular compartments is not a novel occurrence. However, the functions they fulfill tend to be disparate. While cytoplasmic ACL provides acetyl-CoA for lipogenesis, the nuclear isoform participates in the modulation of gene expression via its ability to modulate acetyl-CoA, a key substrate of HATs [1]. Another enzyme that has a multi-organellar presence is LDH. It has been reported in the cytoplasm, mitochondrion and nucleus [11–13]. The cytoplasmic isoform essentially mediates the conversion of pyruvate to lactate with the concomitant conversion of NADH to NAD^+, a process pivotal during anaerobic respiration [14]. In the mitochondrion, LDH provides pyruvate, a moiety involved in a variety of functions, including the production of energy [11]. Although this enzyme has also been found in the nucleus, usually associated with chromatin, its precise role has yet to be fully elucidated [15]. Here,

* Corresponding author. Fax: +1 (705) 675 4844.
E-mail address: vappanna@laurentian.ca (V.D. Appanna).

http://dx.doi.org/10.1016/j.bbrc.2014.10.071
0006-291X/

we report on the ability of nLDH to promote histone deacetylation by modulating the availability of NAD^+.

2. Materials and methods

2.1. Cell culturing and inhibition experiments

HepG2 cells were maintained in α-MEM supplemented with 5% fetal bovine serum (FBS). Cells were seeded at 1×10^5 cells/mL in 175 cm^2 culture flasks and grown in an incubator kept at 37 °C with a 5% CO_2-humidified atmosphere [16]. At 70% confluency HepG2 cells were utilized for various experiments. Media were removed and cells were washed with PBS. The hepatocytes were re-supplemented with serum-free media containing varying amounts of H_2O_2 (10 μM, 40 μM, 60 μM, 80 μM, 100 μM) for 24 h. Forty mM oxamate was added to inhibit LDH and 10 mM nicotinamide was used to inhibit sirtuin activity. Human LDHA-targeted siRNA (Santa Cruz Biotechnology, Inc) was applied according to the manufacturer's protocol. Centrifugation at 150*g* separated the cells from the media. The cell pellet was washed twice in phosphate buffered saline then re-suspended in 1 mL of ice cold mammalian cell storage buffer and stored at −80 °C [16]. To isolate nuclei for experimentation, frozen cells were thawed then centrifuged at 400*g* for 10 min at 4 °C. The cells were then resuspended in 100 μL ice cold mammalian cell storage buffer (MCSB) and homogenized on ice with a sonic dismembrator at an amplitude of 26% and a setting of 1 s bursts for 5 s. The sonication process was repeated 3 times and the suspension was centrifuged at 250 g for 10 min to remove any whole cells. Subcellular components were removed using differential centrifugation. Centrifugation at 800 g for 20 min at 4 °C afforded a nuclear pellet. The pellet was resuspended in 50 μL MCSB before being processed for experimentation. Nuclear purity was ascertained by analyzing histone H2A and actin expression levels in the cellular fractions via Western blot.

2.2. Fluorescence microscopy

Cells were grown on glass coverslips in a 35 mm × 10 mm petri plate. These were seeded at a density of 1×10^5 cells/mL in 2 mL of α-MEM + 5% FBS. Cells were grown to 60–70% confluency, treated with H_2O_2 as described previously and fluorescence microscopy was performed [17]. The cover slips were then exposed to the primary antibody [anti-LDH (1:750), anti-SIRT1 (1:200), anti-acetyl-lysine (1:200)] for 1 h with gentle agitation. Following primary antibody incubation the cells were washed three times with TBS for 5 min and then exposed to the appropriate secondary antibody [anti-goat FITC (1:200), anti-rabbit FITC (1:200)]. After 1 h the secondary antibodies were washed away with TBS three times. Coverslips were mounted on slides and Hoechst and FITC were detected at $\lambda_{excitation}$ = 355 nm and $\lambda_{emission}$ = 465 nm, $\lambda_{excitation}$ = 495 nm and $\lambda_{emission}$ = 520 nm respectively.

2.3. HPLC analysis

Samples were injected into a C_{18}-reverse phase column (Phenomenex) working at a flow rate of 0.7 ml/min. The mobile phase consisted of 20 mM KH_2PO_4 (pH 2.9 with 6 N HCl). The HPLC (Alliance) was calibrated by a 5-point calibration method. Metabolites and protein concentration were determined as described in [11,16]. The utilization of NAD^+ in the nucleus was determined by incubating 2 mg/mL nuclear protein equivalent with 0.5 mM NAD^+ for varying amounts of time at 37 °C in reaction buffer [25mMTris–HCl,5mMMgCl2(pH7.4)] before being loaded into the HPLC for analysis.

2.4. Histone acetylation analyses

Extraction and purification of histones were performed as outlined in [18]. In order to determine the amount of acetylation, histones were hydrolyzed in 6 N H_2SO_4 at 100 °C for 5 h [19]. Following hydrolysis, samples were prepared for HPLC analysis as described previously.

2.5. Blue native polyacrylamide gel electrophoresis (BN-PAGE) and in-gel activity assays

BN PAGE was performed as described in [16,20]. Gradient gels (4–16%) were preferentially used for these assays. LDH activity was assessed as described [21]. Once activity bands were observed the reaction was stopped by adding destaining solution to the reaction (50% methanol, 10% glacial acetic acid). Equal protein loading was ensured by Bradford assay and by running a gel with the same samples and staining with Coomassie blue R-250.

2.6. SDS PAGE and Western blotting

Nuclear protein prepared from control and H_2O_2-treated conditions were prepared with 6x sample buffer [62.5 mM Tris–HCl, 2% (w/v) SDS, 2% (v/v) β-mercaptoethanol (pH 6.8)]. Western blotting was performed as described [21]. Primary antibodies were goat polyclonal to LDH (1:750, Abcam) and rabbit polyclonal to SIRT1 (1:1000, Abcam). Secondary antibodies consisted of donkey anti-goat infrared (IR) 800-conjugated (LI-COR) and goat anti-rabbit IR 600-conjugated (LI-COR), respectively. Detection of the immunoblots was documented using an Odyssey Infrared Imager and accompanying software (LI-COR. Lincoln, NE, USA) [21].

2.7. Co-immunoprecipitation of LDH and SIRT1

Co-immunoprecipitation was performed according to the manufacturer's instructions (Abcam). Nuclei were lysed in 100 μL lysis buffer (1% maltoside, 1 mg/mL BSA, pepstatin A, leupeptin) for 60 min on ice with occasional vortexing. Agarose anti-IgG conjugates were prepared by diluting them 1:1 in dilution buffer (1% maltoside, 1 mg/mL BSA). Twenty microliters of polyclonal anti-LDH was added to the diluted nuclear lysate for 1hr at 4 °C with gentle shaking. Following incubation with the primary antibody, 50 μL of Agarose IgG conjugate was added per tube and allowed to incubate for 1hr with gentle shaking at 4 °C. Following incubation samples were centrifuged at 200 g for 5 s. The supernatant was removed and the pellet was re-suspended in 500 μL of dilution buffer then centrifuged again at 200 g for 5 s. The supernatant was removed and the pellet was re-suspended in TBS and centrifuged. Re-suspension and centrifugation was repeated one more time using a solution of 0.5 M Tris at a pH of 6.8. The pellet was re-suspended in SDS–PAGE sample buffer and heated for 5 min at 100 °C. The sample was centrifuged at 200*g* for 5 s and the supernatant was loaded onto a 10% SDS gel. A Western blot was performed on SIRT1 as described above.

2.8. Statistical analysis

All experiments were performed at least three times and in biological duplicate. Where appropriate, the Student *T* test was utilized to assess significance. A confidence interval of 95% was chosen.

3. Results

3.1. Reactive oxygen species provoke an increase in nuclear LDH

As part of our ongoing effort to decipher the effects of environmental stressors on central metabolism, we treated a human hepatocyte cell line (HepG2) with hydrogen peroxide (H_2O_2), a well-known reactive oxygen species (ROS) that triggers oxidative damage [22]. We investigated the activity of nLDH via blue native polyacrylamide gel electrophoresis (BN-PAGE). In the presence 40 μM H_2O_2 in the culture medium, this enzyme showed a stark increase in activity compared to the control cells, a finding that was found to increase with increasing concentrations of H_2O_2 (Fig. 1A and B). To ascertain the nature of this enzyme, the activity band obtained from nuclear extracts of the H_2O_2-stressed cells was excised and incubated in a reaction mixture containing lactate and NAD^+ and the consumption of the former was monitored by HPLC (Fig. 1C). Indeed, the disappearance lactate peak with the concomitant appearance of a peak attributable to pyruvate after 10 min of incubation further pointed to LDH as a component of the nuclear extract.

3.2. LDH localization and inhibition studies

The discovery of LDH in the nucleus and its dependence on different concentrations of H_2O_2 prompted the further characterization of nLDH and its role in this compartment. To examine whether or not LDH activity was higher in the H_2O_2-treated cultures because of post-translational modification or due to higher expression of the enzyme, fluorescence microscopy and Western blot analyses were performed. LDH expression was unequivocally higher in the nuclear extracts from the H_2O_2-exposed hepatocytes (Fig. 1D). Indeed, Western blots performed on the nuclear fractions further confirmed this finding (Fig. 2A). Five LDH isoenzymes have been characterized. Each enzyme consists of either subunit A or subunit B or a mixture of both [23]. Nuclear LDH is commonly referred to as LDH5 (A_4), comprised solely of the A subunit [24]. To identify whether or not this specific isoenzyme was an A-containing LDH, we used $AgNO_3$ to inhibit any LDH enzymes containing subunit A [11,25]. The abolition of the bands from the in-gel activity assay when $AgNO_3$ was included in the reaction mixture indicated that the nuclear isoenzyme of LDH in this study did indeed have subunit A (Fig. 2B). LDHA preferentially converts pyruvate to lactate, regenerating NAD^+ in the process [23].

3.3. Histone acetylation is lower in H_2O_2-treated HepG2 cultures

As nLDH and NAD^+ production were higher in the nucleus of the H_2O_2-challenged hepatocytes, the significance of this enhanced NAD^+ was examined. The nuclear extracts were incubated with NAD^+ and its utilization was monitored. The results revealed that NAD^+ was being consumed faster in the stressed nuclei than in the control (Fig. 2C). As sirtuin-fueled NAD^+ consumption is known to promote histone deacetylation, histones were isolated from the nuclei under control and H_2O_2-stressed conditions and hydrolyzed

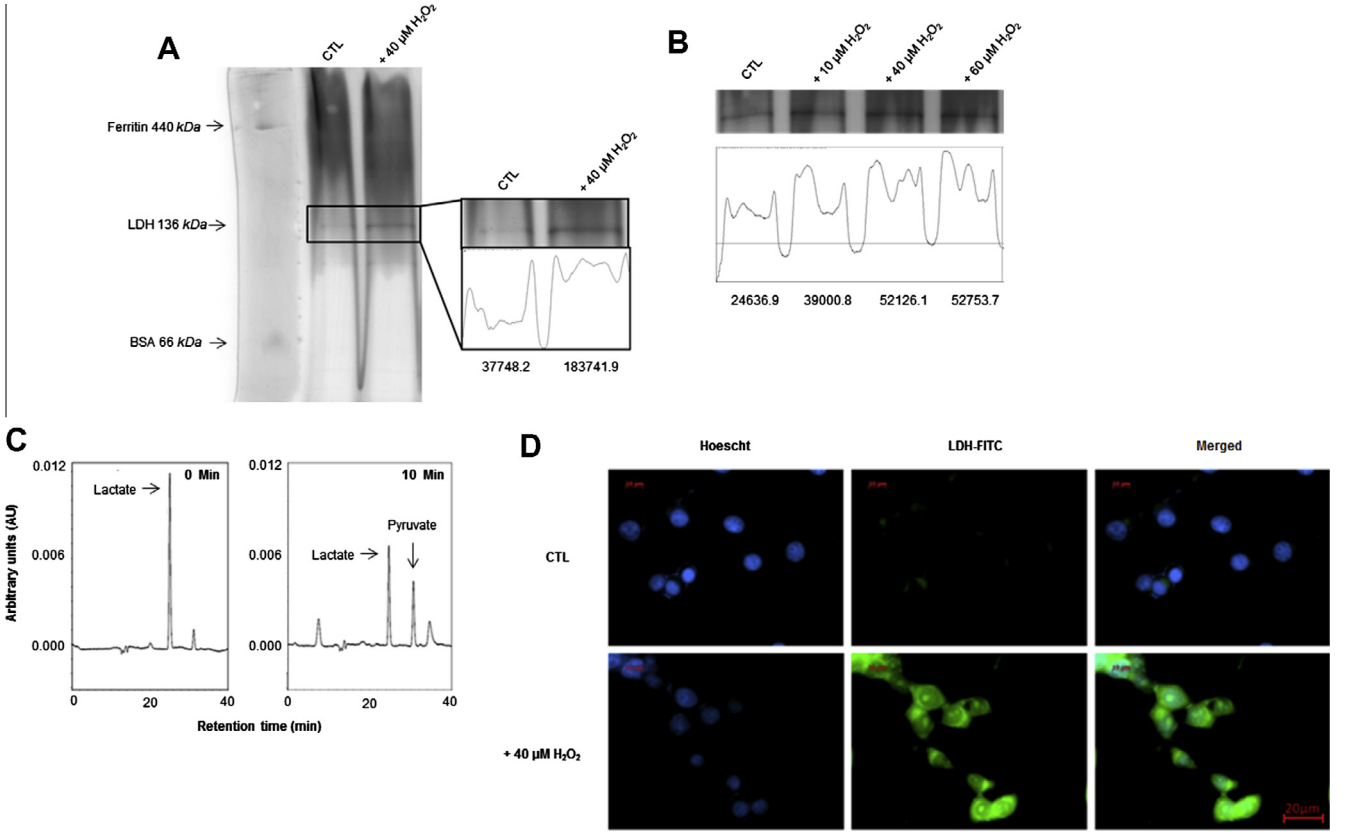

Fig. 1. Hydrogen peroxide stress results in increased nuclear LDH activity in hepatocytes. (A) Proteins were run in a BN-PAGE gel and nLDH activity was ascertained. A representative gel is shown ($n = 3$). Densitometry was assessed using ImageJ for Windows. (B) Increasing concentrations of H_2O_2 were utilized to ascertain the dose-dependence of nLDH. (C) The nLDH activity band was excised and incubated with 2 mM lactate and 0.1 mM NAD^+ for 10 min. The disappearance of lactate and appearance of pyruvate were monitored via HPLC. A representative chromatogram is shown ($n = 3$; H2A and actin were probed prior to activity assays to ascertain the purity of nuclear extracts). (D) Representative micrograph ($n = 3$) utilized to demonstrate the nuclear localization of LDH. Cells were grown on coverslips in two groups, control and stress. A primary anti-LDH antibody was applied with a secondary conjugated to the fluorescent tag FITC. Hoechst was used as a counterstain to visualize the nucleus. The cells were observed on a deconvolution fluorescent microscope.

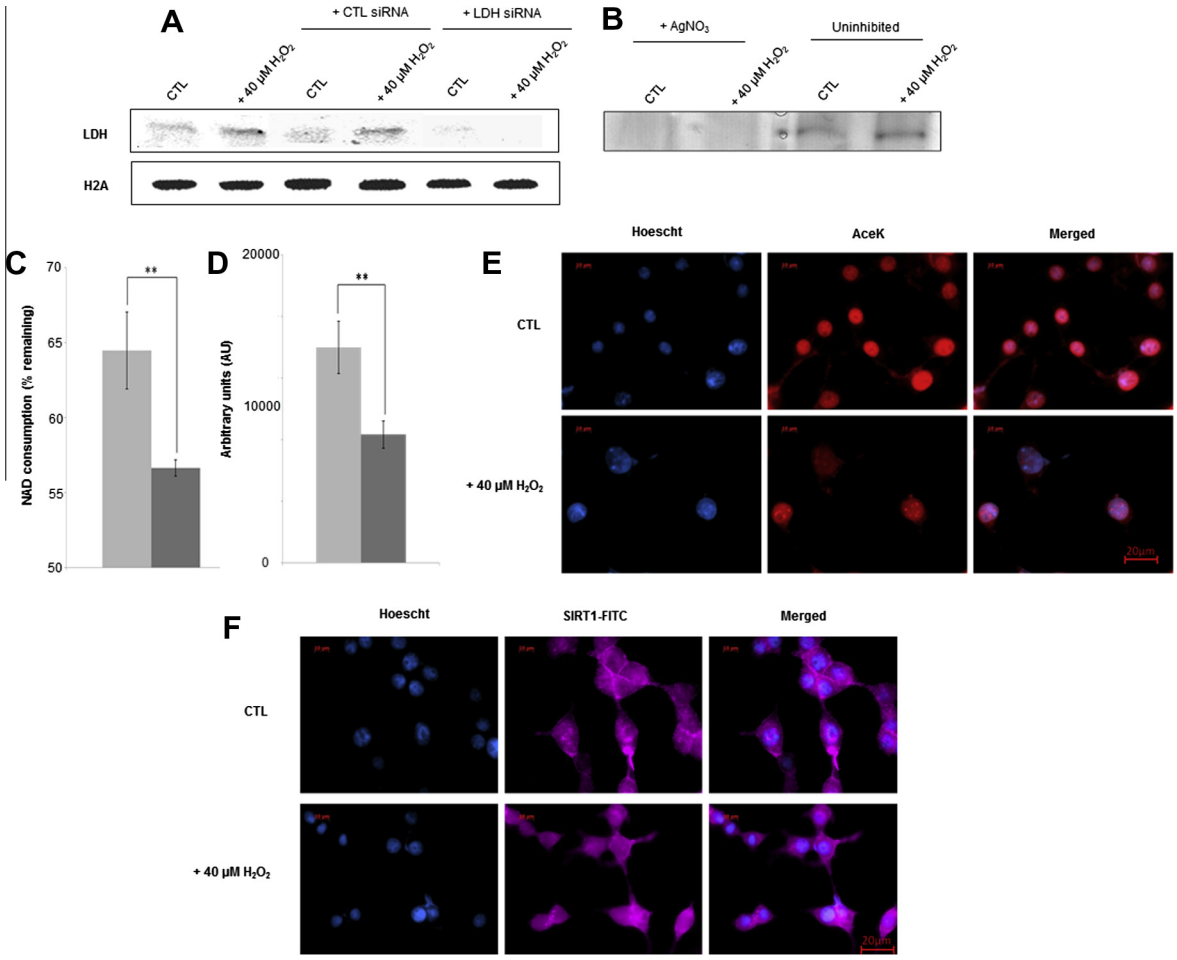

Fig. 2. Nuclear LDH and histone deacetylation. (A) Nuclei were extracted from control and H_2O_2-stressed hepatocytes and a Western blot was performed with antibodies targeting LDH5. The experiment was repeated with cells treated with CTL siRNA as well as siRNA targeting LDH. Antibodies versus H2A were used as a loading control. (B) An activity assay was performed for LDH in the presence or absence of 2 mM $AgNO_3$ to determine if the LDH in question contained subunit A ($n = 3$; Ctl = Control). (C) Whole nuclei isolated from control (□) and H_2O_2-stressed (■) cells were incubated with 2 mM NAD^+ for one hour at 37 °C. Samples were boiled to stop any reactions and the amount of NAD^+ left compared to time zero was analyzed via HPLC ($n = 3 \pm SD$; $P \leqslant 0.01$). (D) Histones were isolated from the nucleus of control (□) and H_2O_2-stressed (■) cells and hydrolyzed to liberate acetate. The latter was measured by HPLC using a reverse phase C-18 column at a flow rate of 0.7 mL/min for 30 min ($n = 3 \pm SD$; $P \leqslant 0.01$). (E) Control and stressed cells were grown on glass coverslips until 70% confluent. After stressing with H_2O_2, fluorescence microscopy was performed using Hoechst as a counter stain to visualize the nucleus and primary antibodies targeting acetylated. Lysine residues with secondaries conjugated to FITC. This is a representative micrograph ($n = 3$). (F) After stressing with H_2O_2, fluorescence microscopy was performed using an anti-SIRT1 primary antibody coupled to a FITC-tagged secondary antibody to visualize SIRT1. A deconvolution microscope was used to visualize the cells after staining. This is a representative micrograph ($n = 3$).

to liberate the acetate moieties. Indeed, levels of this monocarboxylic acid were significantly lower in the H_2O_2-treated cells (Fig. 2D). This finding was further confirmed by fluorescence microscopy using antibodies generated against acetylated lysine residues, moieties commonly found on histones. Under H_2O_2 stress, lower amounts of acetylated histones were detected (Fig. 2E). To assess whether these fluctuations in histone acetylation under stress were due to changes in the expression of SIRT1, the levels of this enzyme were verified by fluorescence microscopy. There appeared to be no significant change in the concentration of SIRT1, thus supporting the notion that the expression of this enzyme was not influencing histone acetylation (Fig. 2F). The unchanged levels of SIRT1 coupled with the increased expression of nLDH and the rapid utilization of NAD^+ in the H_2O_2-challenged cells pointed to the role of nLDH in modulating histone deacetylation by controlling the NAD^+ availability.

3.4. Nuclear LDH supplies NAD^+ for the epigenetic modification of histones

To confirm this hypothesis, experiments were performed to assess the effects of selective inhibitors on histone acetylation and the nuclear metabolic profile. LDH activity was arrested with the aid of the competitive inhibitor oxamate, a moiety with structural similarity to pyruvate, the preferential substrate of LDH5 [11,26]. Isolation of histones followed by hydrolysis and analysis of acetate levels via HPLC revealed that there was less of this metabolite than in untreated cells. Additionally, the level of acetate on histones from the H_2O_2-treated cultures approached that of the control cultures upon treatment with oxamate, thus implicating nLDH in this epigenetic modification (Fig. 3A). To further support this observation, siRNA targeting LDH was transfected into the HepG2 cell line. The knock down of this enzyme produced similar results to those observed with the chemical inhibitor oxamate (Fig. 3B).

3.5. SIRT1 and nLDH act in tandem to modulate histone acetylation

When SIRT1 activity was suppressed using the noncompetitive inhibitor nicotinamide, there was a pronounced variation in the levels of histone acetylation when compared to uninhibited hepatocytes (Fig. 3C) [27]. This was an intriguing finding, suggesting interplay between SIRT1 and nLDH. The perturbation in the levels of these metabolites in the nucleus upon inhibition of SIRT1

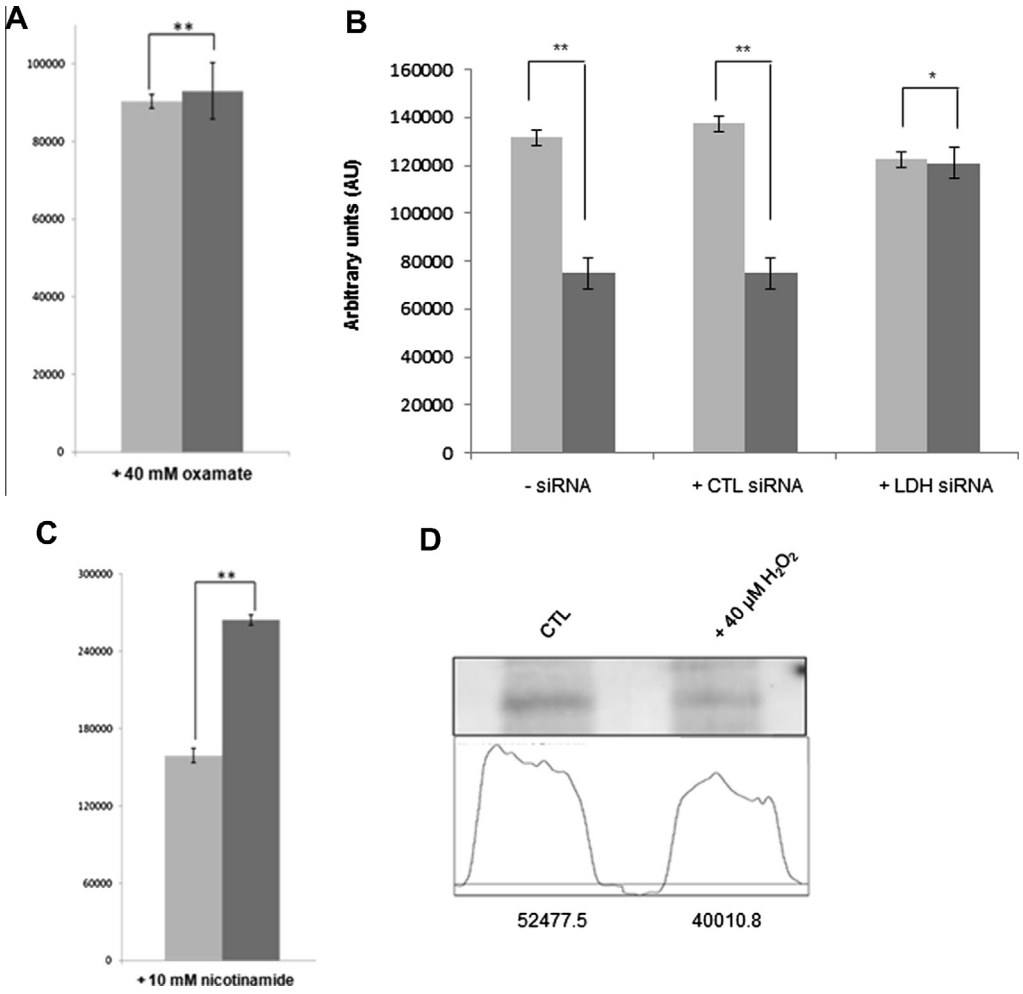

Fig. 3. Nuclear LDH and SIRT1 act in tandem to modulate gene expression. (A) Oxamate (40 mM), an inhibitor of LDH, was added to the medium. Histones were then isolated from the nucleus of control (□) and H_2O_2-stressed (■) cells and hydrolyzed to liberate acetate. The latter was measured by HPLC ($n = 3 \pm SD$; $P \leqslant 0.01$). (B) HepG2 cells from control and stress groups were incubated with CTL or LDH-targeted siRNA. Histones were then isolated from the nucleus of control (□) and H_2O_2-stressed (■) cells and hydrolyzed to liberate acetate. The latter was measured by HPLC ($n = 3 \pm SD$; $^{*}P \leqslant 0.05$; $^{**}P \leqslant 0.01$). (C) Nicotinamide (10 mM), an inhibitor of SIRT1, was added to the medium. Histones were then isolated from the nucleus of control (□) and H_2O_2-stressed (■) cells and hydrolyzed to liberate acetate. The latter was measured by HPLC ($n = 3 \pm SD$; $P \leqslant 0.01$). (D) Anti-LDH antibodies were used to pull down SIRT1 in both the control and stressed cells. Bands were present at 120 kDA following immunoblotting with antibodies against SIRT1. A representative blot ($n = 3$) is depicted. Densitometry was assessed using ImageJ for Windows.

indicated a link between LDH, the modulation of NAD^+ and the deacetylase. These observations prompted us to explore whether SIRT1 had any direct interactions with nLDH that may facilitate the shuttling of the crucial cofactor NAD^+ to SIRT1. The known association of both sirtuins and LDH5 with chromatin in addition to the fact that HDACs function in multimolecular complexes led to the notion that nuclear LDH and sirtuins may exist as part of the same protein complex [28]. Pull-down studies using antibodies against LDH successfully co-immunoprecipitated SIRT1 at its predicted molecular mass of 120 kDa, as visualized by Western blot (Fig. 3D). This intimate association between the two nuclear enzymes would indeed facilitate metabolic channeling and the subsequent epigenetic modification in the nucleus.

4. Discussion

Although the roles of enzymes such as nACL and NAMPT are now beginning to emerge, nuclear metabolism and its role in the translation of genetic information has yet to be fully appreciated. The results described in this report point to a novel function of the nucleus-residing LDH. The data suggest a link between ROS stress, nLDH and epigenetic modifications. Confronted by the H_2O_2 challenge, hepatocytes opt to increase the expression of LDH in the nucleus in order to produce NAD^+, an essential ingredient for SIRT1 activity. Pyruvate may be pooled in the cytosol under oxidative stress and transported to the nucleus to serve as substrate for nLDH. Indeed, previous studies have indicated that ROS toxicity leads to the inactivation of pyruvate dehydrogenase (PDH), aconitase (ACN), and other tricarboxylic acid (TCA) cycle enzymes, conditions conducive to the accumulation of this monocarboxylic acid [29]. The intimate association between nLDH and SIRT1 in the nucleus would ensure that NAD^+ is readily available for histone deacetylation, an event effecting the transmission of genetic information (Fig. 4).

The ability to signal the nucleus via central metabolism is critical for proper cellular functioning. The foregoing data illustrate how metabolic cues may be transmitted to the nucleus with the aid of such participants as pyruvate, NAD^+ and LDH. Upon exposure to ROS stress, the needs of a cell drastically change from that of energy production to combating ROS stress and limiting the formation of these toxic species. Central metabolism can respond immediately to these changes via key ROS sensing enzymes like alpha-ketoglutarate dehydrogenase and PDH [30]. The inactivation

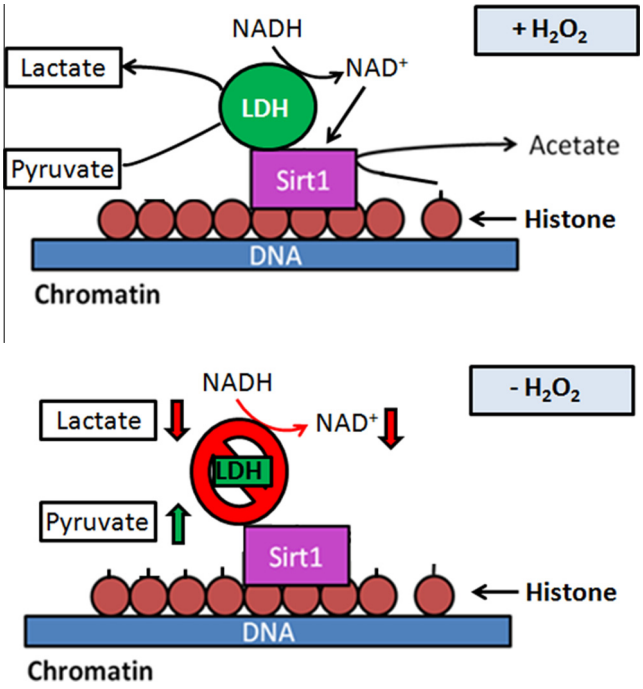

Fig. 4. A scheme depicting how nuclear LDH orchestrates epigenetic changes in hepatocytes. Scheme depicting the connection between LDH and SIRT1, a phenomenon conducive to the deacetylation of histones and a proposed link between metabolism and gene regulation. ▮ = acetyl group.

of the sulfhydryl moiety in these enzymes results in the increase of metabolites like pyruvate that subsequently enables a shift in the NAD^+ gradient in the nucleus. The latter event mediated by nLDH and the ensuing biochemical response fuels epigenetic changes. Hence, nLDH is a critical link in this cellular conversation aimed at connecting metabolic networks to the transmission of genetic information.

Acknowledgments

This work was supported by Laurentian University and Industry Canada. Christopher Auger is a recipient of the NSERC PGS-D. Sean Thomas is a recipient of the Ontario Graduate Scholarship.

References

[1] K.E. Wellen, G. Hatzivassiliou, U.M. Sachdeva, T.V. Bui, J.R. Cross, C.B. Thompson, ATP-citrate lyase links cellular metabolism to histone acetylation, Science 324 (2009) 1076–1080.
[2] A.A. Sauve, C. Wolberger, V.L. Schramm, J.D. Boeke, The biochemistry of sirtuins, Annu. Rev. Biochem. 75 (2006) 435–465.
[3] A.M. Kalle, A. Mallika, J. Badiger, C. Alinakhi, P. Talukdar, D. Sachchidanand, Inhibition of SIRT1 by a small molecule induces apoptosis in breast cancer cells, Biochem. Biophys. Res. Commun. 401 (2010) 13–19.
[4] S.Y. Jang, H.T. Kang, E.S. Hwang, Nicotinamide-induced mitophagy: event mediated by high NAD^+/NADH ratio and SIRT1 protein activation, J. Biol. Chem. 287 (2012) 19304–19314.
[5] D.J. Bonda, H.G. Lee, A. Camins, M. Pallàs, G. Casadesus, M.A. Smith, X. Zhu, The sirtuin pathway in ageing and Alzheimer disease: mechanistic and therapeutic considerations, Lancet Neurol. 10 (2011) 275–279.
[6] M. Yamamoto, G. Iguchi, H. Fukuoka, K. Suda, H. Bando, M. Takahashi, H. Nishizawa, S. Seino, Y. Takahashi, SIRT1 regulates adaptive response of the growth hormone–insulin-like growth factor-I axis under fasting conditions in liver, Proc. Natl. Acad. Sci. U.S.A. 110 (2013) 14948–14953.
[7] V. Guarani, G. Deflorian, C.A. Franco, M. Krüger, L.K. Phng, K. Bentley, L. Toussaint, F. Dequiedt, R. Mostoslavsky, M.H. Schmidt, et al., Acetylation-dependent regulation of endothelial Notch signalling by the SIRT1 deacetylase, Nature 473 (2011) 234–238.
[8] A. Menssen, P. Hydbring, K. Kapelle, J. Vervoorts, J. Diebold, B. Lüscher, L.G. Larsson, H. Hermeking, The c-MYC oncoprotein, the NAMPT enzyme, the SIRT1-inhibitor DBC1, and the SIRT1 deacetylase form a positive feedback loop, Proc. Natl. Acad. Sci. U.S.A. 109 (2012) 187–196.
[9] T. Zhang, J.G. Berrocal, K.M. Frizzell, M.J. Gamble, M.E. DuMond, R. Krishnakumar, T. Yang, A.A. Sauve, W.L. Kraus, Enzymes in the NAD^+ salvage pathway regulate SIRT1 activity at target gene promoters, J. Biol. Chem. 284 (2009) 20408–20417.
[10] T.F. Liu, B.K. Yoza, M. El Gazzar, V.T. Vachharajani, C.E. McCall, NAD^+-dependent SIRT1 deacetylase participates in epigenetic reprogramming during endotoxin tolerance, J. Biol. Chem. 286 (2011) 9856–9864.
[11] J. Lemire, R.J. Mailloux, V.D. Appanna, Mitochondrial lactate dehydrogenase is involved in oxidative-energy metabolism in human astrocytoma cells (CCF-STTG1), PLoS ONE 3 (2008) e1550.
[12] A. Cattaneo, S. Biocca, N. Corvaja, P. Calissano, Nuclear localization of a lactic dehydrogenase with single-stranded DNA-binding properties, Exp. Cell Res. 161 (1985) 130–140.
[13] T. Hashimoto, R. Hussien, G.A. Brooks, Colocalization of MCT1, CD147, and LDH in mitochondrial inner membrane of L6 muscle cells: evidence of a mitochondrial lactate oxidation complex, Am. J. Physiol. Endocrinol. Metab. 290 (2006) 1237–1244.
[14] J.T. Newington, T. Rappon, S. Albers, D.Y. Wong, R.J. Rylett, R.C. Cumming, Overexpression of pyruvate dehydrogenase kinase 1 and lactate dehydrogenase A in nerve cells confers resistance to amyloid beta and other toxins by decreasing mitochondrial respiration and reactive oxygen species production, J. Biol. Chem. 287 (2012). 37245-32758.
[15] X.H. Zhong, B.D. Howard, Phosphotyrosine-containing lactate dehydrogenase is restricted to the nuclei of PC12 pheochromocytoma cells, Mol. Cell. Biol. 10 (1990) 770–776.
[16] R.J. Mailloux, V.D. Appanna, Aluminum toxicity triggers the nuclear translocation of HIF-1alpha and promotes anaerobiosis in hepatocytes, Toxicol. In Vitro 21 (2007) 16–24.
[17] J. Lemire, R. Mailloux, S. Puiseux-Dao, V.D. Appanna, Aluminum-induced defective mitochondrial metabolism perturbs cytoskeletal dynamics in human astrocytoma cells, J. Neurosci. Res. 87 (2009) 1474–1483.
[18] D. Shechter, H.L. Dormann, C.D. Allis, S.B. Hake, Extraction, purification and analysis of histones, Nat. Protoc. 2 (2007) 1445–1457.
[19] D.M. Phillips, The presence of acetyl groups of histones, Biochem. J. 87 (1963) 258–263.
[20] H. Schagger, G. von Jagow, Blue native electrophoresis for isolation of membrane protein complexes in enzymatically active form, Anal. Biochem. 199 (1991) 223–231.
[21] J. Lemire, C. Auger, R.J. Mailloux, V.D. Appanna, Mitochondrial lactate metabolism is involved in antioxidative defense in human astrocytoma cells, J. Neurosci. Res. 92 (2014) 464–475.
[22] Y. Zhang, C.G. Tocchetti, T. Krieg, A.L. Moens, Oxidative and nitrosative stress in the maintenance of myocardial function, Free Radic. Biol. Med. 53 (2012) 1531–1540.
[23] W. Eventoff, M.G. Rossmann, S.S. Taylor, H.J. Torff, H. Meyer, W. Keil, H.H. Kiltz, Structural adaptations of lactate dehydrogenase isozymes, Proc. Natl. Acad. Sci. U.S.A. 74 (1977) 2677–2681.
[24] M.I. Koukourakis, A. Giatromanolaki, C. Simopoulos, A. Polychronidis, E. Sivridis, Lactate dehydrogenase 5 (LDH5) relates to up-regulated hypoxia inducible factor pathway and metastasis in colorectal cancer, Clin. Exp. Metastasis 22 (2005) 25–30.
[25] J. Schmitt, H. Ritter, Lactate dehydrogenase: inhibition of subunit A by the sulfhydryl reagent $AgNO_3$, Humangenetik 28 (1975) 239–243.
[26] S. McClendon, D.M. Vu, K. Clinch, R. Callender, R.B. Dyer, Structural transformations in the dynamics of Michaelis complex formation in lactate dehydrogenase, Biophys. J. 89 (2005) 07–09.
[27] J.L. Avalos, K.M. Bever, C. Wolberger, Mechanism of sirtuin inhibition by nicotinamide: altering the NAD(+) cosubstrate specificity of a Sir2 enzyme, Mol. Cell 17 (2005) 855–868.
[28] L. Ho, G.R. Crabtree, Chromatin remodelling during development, Nature 463 (2010) 474–484.
[29] T.R. Hurd, Y. Collins, I. Abakumova, E.T. Chouchani, B. Baranowski, I.M. Fearnley, T.A. Prime, M.P. Murphy, A.M. James, Inactivation of pyruvate dehydrogenase kinase 2 by mitochondrial reactive oxygen species, J. Biol. Chem. 287 (2012) 35153–35160.
[30] L.J. Yan, N. Sumien, N. Thangthaeng, M.J. Forster, Reversible inactivation of dihydrolipoamide dehydrogenase by mitochondrial hydrogen peroxide, Free Radic. Res. 47 (2013) 123–133.